ADVANCED ELECTROMAGNETICS, Vol. 1, No. 1, May 2012

Broadband impedance spectroscopy of some Li^+ and $V_O^{\bullet\bullet}$ conducting solid electrolytes

Antanas Feliksas Orliukas[1], Odile Bohnke[2], Algimantas Kežionis[1], Saulius Kazlauskas[1], Vilma Venckutė[1], Dalius Petrulionis[1], Tomas Žukauskas[1], Tomas Šalkus[1], Antonija Dindune[3], Zaiga Kanepe[3], Janis Ronis[3], Vytautas Kunigėlis[1]

[1]Faculty of Physics, Vilnius University, Saulėtekio al. 9/3, LT-10222 Vilnius, Lithuania
[2] Laboratoire des Oxydes et Fluorures UMR 6010 CNRS Institut des Molécules et Matériaux du Mans (I3M) Université du Maine, Avenue Olivier Messiaen 72085 Le Mans Cedex 9
[3] Institute of Inorganic Chemistry, Riga Technical University, Miera iela 34, 2169 Salaspils, Latvia
*corresponding author, E-mail: tomas.salkus@ff.vu.lt

Abstract

The solid electrolyte $Li_3Ti_{1.5}(PO_4)_3$ compound has been synthesized by solid state reaction and studied by X-ray diffraction. At room temperature the compound belongs to rhombohedral symmetry (space group $R\bar{3}c$) with six formula units in the unit cell. $Li_3Ti_{1.5}(PO_4)_3$, $Li_{3x}La_{2/3-x}TiO_3$ (where x = 0.12) Li^+-ion conducting, $Ce_{0.8}Gd_{0.2}O_{1.9}$, $(ZrO_2)_{92}(Y_2O_3)_8$ with fast oxygen vacancy transport ceramic samples were investigated in the frequency range from 1 Hz to 3 GHz in the temperature interval (300-700) K by impedance spectroscopy methods. Two dispersion regions in ionic conductivity spectra for investigated ceramic samples have been found. The dispersions have been attributed to relaxation processes in grain boundaries and in grains of the ceramics.

1. Introduction

The development of fast lithium conductors is attracting much attention because of their potential applications in electrochemical devices such as high-energy lithium ion batteries and electrochemical gas sensors. $Li_{3x}La_{2/3-x}TiO_3$ (LLTO) is known as a fast Li-ion conductor [1, 2]. LLTO has ABO_3 perovskite-type structure. The unit cell is built of TiO_6 octahedra and A-cages are formed by 12 oxygen ions belonging to 8 octahedra [3, 4]. La^{3+} is unequally distributed in the structure forming La-rich and La-poor layers, which open paths for Li^+ migration [4]. The compound $LiTi_2(PO_4)_3$ with NASICON-type framework structure is a pure ionic conductor, its bulk ionic conductivity $\sigma_b = 10^{-4}$ S/m at room temperature [5]. Conductivity increases then Ti^{+4} is partially substituted by three valence state ions in NASICON – type framework [6]. Today, cubic structure zirconia-based materials such as $Zr_{0.85}Ca_{0.15}O_{1.85}$ (15CSZ), $(ZrO_2)_{90}(Y_2O_3)_{10}$ (YSZ10), $(ZrO_2)_{92}(Y_2O_3)_8$ (YSZ8), $Ce_{0.8}Gd_{0.2}O_{1.9}$ (GDC20) with fast oxygen vacancy transport are used for variety of applications, namely oxygen gas sensors, as well as for solid oxide fuel cells (SOFC) [7]. Furthermore, the above mentioned Li^+ and $V_O^{\bullet\bullet}$ conducting solid electrolytes do not undergo any phase transition in the temperature range from room to 1000 K and therefore they are also interesting candidates for ionic dynamics' studies in the broad frequency range of the electric field. In the present work we present investigation results of electrical properties of $Li_3Ti_{1.5}(PO_4)_3$, $Li_{3x}La_{2/3-x}TiO_3$ (with stoichiometric factor x = 0.12), YSZ8, and GDC20 ceramics in the frequency range $(1\text{-}3\cdot10^9)$ Hz in the temperature range (300-700) K by impedance spectroscopy methods. The preparation conditions of $Li_3Ti_{1.5}(PO_4)_3$ powder and ceramics, the results of the X-ray diffraction (XRD) study are presented in the paper too.

2. Experiment

The powder of $Li_3Ti_{1.5}(PO_4)_3$ has been synthesized from stoichiometric mixture of Li_2CO_3 (purity 99.999 %), extra pure $NH_4H_2PO_4$ and TiO_2 by solid state reaction. The mixture with stoichometric amounts was placed in ethyl alcohol and milled 8 hours in an agate mill. After milling the mixture was heated for 20 h at temperature $T = 723$ K. After heating the mixture was placed in the ethyl alcohol and this liquid was milled 8 h in the planetary mill again. After this process the powder was heated for 8 h at $T = 1173$ K. The fine powder was dried at $T = 393$ K for 24 h. The structure parameters were obtained using Brucker D8 Advance equipment at room temperature from the X-ray powder diffraction patterns in the region $2\Theta = 6\text{-}80$ degree, step 0.02 degree, time per step 1-8 sec., $CuK_{\alpha 1}$ radiation (40 kV, 40 mA). The lattice parameters were deduced by fitting the XRD patterns with software TOPAS. For investigation of electrical properties the ceramic samples were sintered. The powder was uniaxially cold-pressed at 300 MPa. The sintering of $Li_3Ti_{1.5}(PO_4)_3$ ceramic samples was conducted in air at $T = 923$ K. The sintering duration of the ceramics was 1 h. The density of so sintered $Li_3Ti_{1.5}(PO_4)_3$ ceramic samples was $d = 2.48$ g/cm^3.

The conditions of the preparation of LLTO powder can be found elsewhere [8]. To obtain LLTO (x = 0.12) ceramics with grain sizes in the range of micrometers conventional

solid state reaction was used and the obtained powder has been pressed and sintered at 1523 K for 2 h. In the current work we name this sample as LLTO - SSR. A modified Pechini-type complex polymerizable method was used to obtain LLTO (x = 0.12) powder with grains in the nanometer range (20 – 30 nm). Ceramic samples from nano-powders have been sintered in this way: The pressed pellets were introduced into hot oven (1373 K), kept for 3 min and quenched to room temperature. Such procedure leads to formation of dense ceramics (relative density was more than 90 %) with limited grain growth. In our current work we name nano-ceramics as LLTO - P.

YSZ8 and GDC20 ceramics have been sintered at 1773 K for 2 h using the fine powder from Fuel Cell Materials.

The measurements of complex conductivity ($\tilde{\sigma} = \sigma' + \mathrm{i}\sigma''$), complex specific electrical resistivity ($\tilde{\rho} = \rho' - \mathrm{i}\rho''$), and complex dielectric permittivity ($\tilde{\varepsilon} = \varepsilon' - \mathrm{i}\varepsilon''$) were performed in temperature range from 300 K to 700 K. Platinum electrodes were prepared on investigated samples by applying Pt paste (GVENT Electronic Materials LTD) fired at 1073 K except for both LLTO samples, where thin sputtered gold electrodes have been used. For measurements of electrical impedance in the frequency range ($1\text{-}1\cdot10^6$) Hz four-probe method was used. The measurements in the frequency range ($3\cdot10^5\text{-}3\cdot10^9$) Hz were performed by Agilent Network Analyzer E5062A connected to coaxial line, the part of inner conductor of which was replaced by the sample. The impedance of the sample was calculated from scattering parameters' matrix of two port network as in [9]. The temperature of investigated materials in the low and high frequency ranges was measured by K-type thermocouple.

3. Discussion

Fig. 1 shows powder X-ray diffraction patterns of $Li_{1.2}Ti_{1.5}(PO_4)_3$ prepared by solid state reaction. A small amount (up to 1.5 %) of $LiTiO_5$ and $Li_4(P_2O_7)$ were detected as impurities and are marked in Fig. 1. At room temperature $Li_3Ti_{1.5}(PO_4)_3$ compound belongs to the rhombohedral symmetry (space group $R\bar{3}c$) with six formula units in the unit cell. The lattice parameters, unit cell volume (V) and theoretical density (d_t) of the investigated compounds are presented in Table 1.

The impedance spectroscopy investigation of ion-conducting ceramics in the wide frequency and in the broad temperature ranges allows one to separate charge carrier transport processes in grains and in grain boundaries of the ceramics.

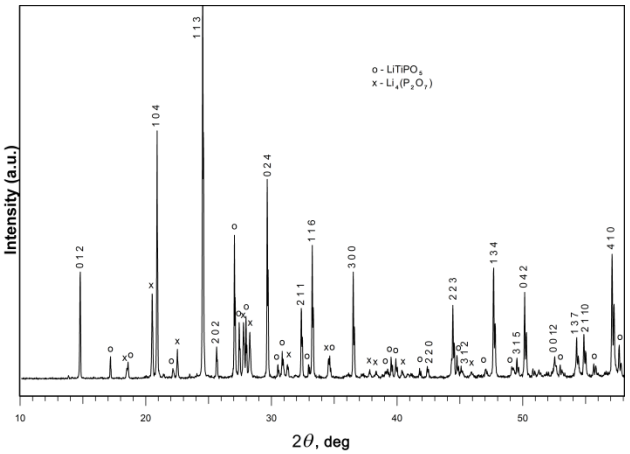

Figure 1: X-ray powder diffraction pattern of $Li_3Ti_{1.5}(PO_4)_3$. o and × mark some impurity peaks. Numbers above the peaks are Miller indices.

In Fig. 2 (a), (b), and (c) the characteristic frequency dependences of the real part (σ') of complex conductivity of $Li_3Ti_{1.5}(PO_4)_3$, LLTO, YSZ8, and GDC20 ceramics measured at different temperatures are shown. Two dispersion regions in σ' spectra for investigated ceramic samples were found. All the processes are thermally activated and dispersion regions shift towards higher frequencies as temperature increases. As it is generally observed in solid electrolyte ceramics [10–15], the high frequency part of the recorded spectra may be attributed to the Li^+-ion or $V_O^{\bullet\bullet}$ relaxation processes in grains, while the lower frequency part corresponds to relaxation processes in grain boundaries. Temperature dependences of total conductivity (σ_{tot}) of the ceramics were derived from dependences of $\sigma'(f)$ measured by four probe method at different temperatures. The temperature dependences of bulk conductivity (σ_b) of the ceramic samples were derived from the complex plots of $\rho''(\rho')$ and $\sigma''(\sigma')$ measured in microwave region at different temperatures. In Fig. 3(a), (b) and (c) the typical complex specific electrical resistivity plots of $Li_3Ti_{1.5}(PO_4)_3$, LLTO ceramic samples at 300 K and YSZ8, GDC20 ceramics at 600 K are shown.

Temperature dependences of σ_{tot} and σ_b of $Li_3Ti_{1.5}(PO_4)_3$, LLTO, YSZ8, and GDC20 ceramic samples are shown in Fig. 4 (a), (b). The activation energies of σ_{tot} and σ_b were found from the slopes of the Arrhenius plots. Table 2 summarizes our experimental results of the investigation of σ_{tot}, σ_b and their activation energies $\Delta E_{\sigma tot}$, $\Delta E_{\sigma b}$.

Table 1: Summary of X-ray diffraction results for $Li_3Ti_{1.5}(PO_4)_3$ compounds at room temperature.

Compound	Symmetry and space group	a, Å	c, Å	V, Å^3	Z	d_t, g/cm^3
$Li_3Ti_{1.5}(PO_4)_3$	Rhombohedral ($R\bar{3}c$)	8.5150	20.8755	1310.80	6	2.85

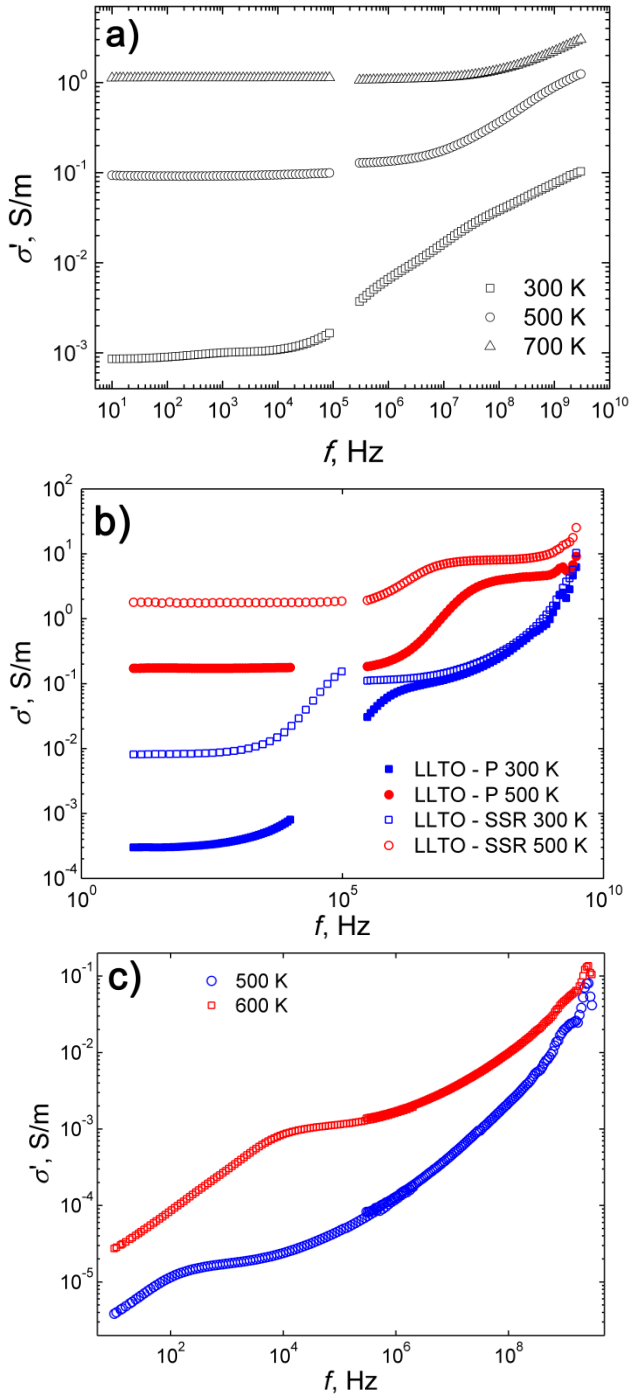

Figure 2: Frequency dependences of the real part of conductivity measured at different temperatures of $Li_3Ti_{1.5}(PO_4)_3$ (a), LLTO - P and LLTO - SSR (b), and 8YSZ (c) ceramics.

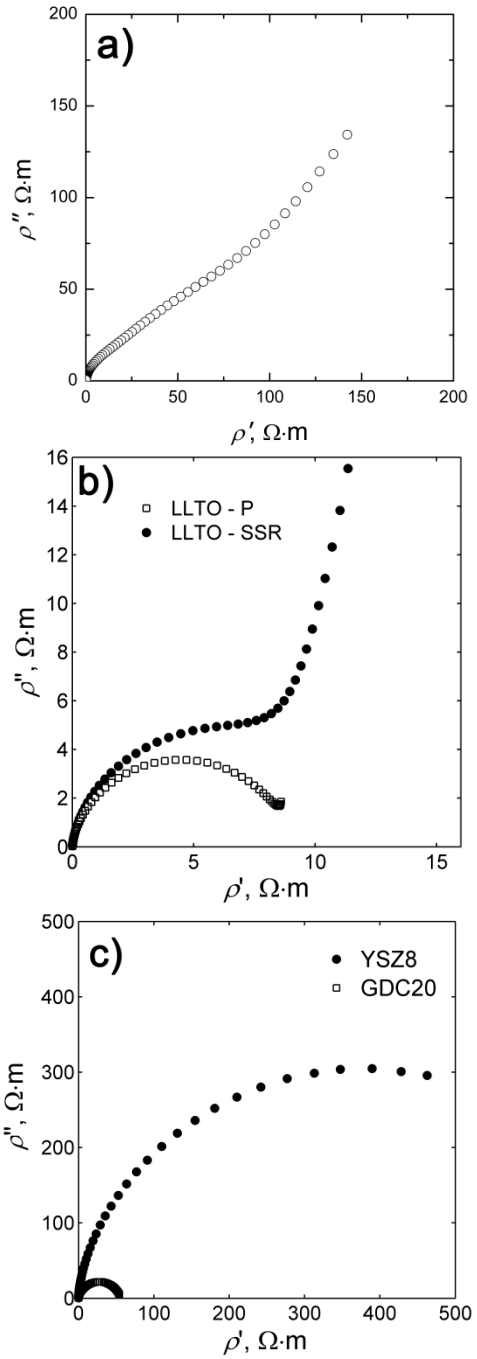

Figure 3: High frequency impedance complex plain plots of: Li3Ti1.5(PO4)3 at 300 K (a), LLTO at 300 K (b), and YSZ8, GDC20 at 600 K (c).

Table 2: σ_{tot}, σ_b, their activation energies and the activation energy of the relaxation frequency in bulk of $Li_3Ti_{1.5}(PO_4)_3$, LLTO ceramic samples at 400 K and GDC20, YSZ8 ceramic samples at 600 K.

Compound	σ_{tot}, S/m	$\Delta E_{\sigma tot}$, eV	σ_b, S/m	$\Delta E_{\sigma b}$, eV	ΔE_f, eV
$Li_3Ti_{1.5}(PO_4)_3$	0.32	0.30	0.02	0.19	0.25
LLTO - SSR	2.1	0.41	0.19	0.28	0.31
LLTO - P	1.4	0.42	0.015	0.25	0.27
GDC20	0.0035	1.12	0.018	0.87	0.93
YSZ8	$8.1 \cdot 10^{-4}$	1.03	0.0013	0.90	1.1

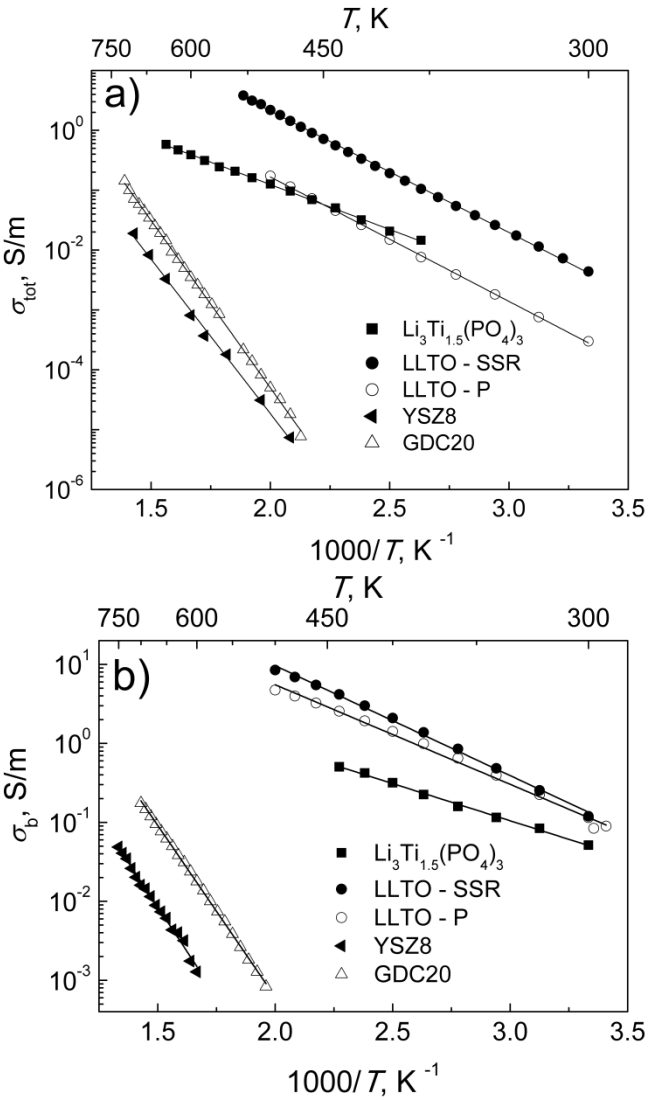

Figure 4: Temperature dependences total (a) and bulk (b) ionic conductivities of the investigated ceramics.

In $Li_3Ti_{1.5}(PO_4)_3$ and LLTO compounds the temperature dependences of the conductivity is caused by Li^+ ion mobility increase in the materials and in YSZ8 and GDC20 ceramics – by oxygen vacancy mobility witch increases as temperature increases. A slight difference of the bulk conductivities and their activation energies can be observed from Fig. 4 when comparing both LLTO samples. These differences probably appear because of different heat treatment of the samples which leads to rearrangement of La-rich and La-poor layers in LLTO. On the other hand, a very big difference can be seen between total ionic conductivities of LLTO - P and LLTO - SSR samples. This feature is typical for LLTO ceramics, for which the total conductivity is lowered because of the low conductivity of boundaries between the ceramic's grains.

From the maxima of $\rho''(f)$ (Fig. 5), Maxwell relaxation frequency ($f_M = \sigma_b/2\pi\varepsilon'\varepsilon_0$, where $\varepsilon_0 = 8.85 \times 10^{-12}$ F/m is dielectric constant) was determined at different temperatures, as described previously in [14-16].

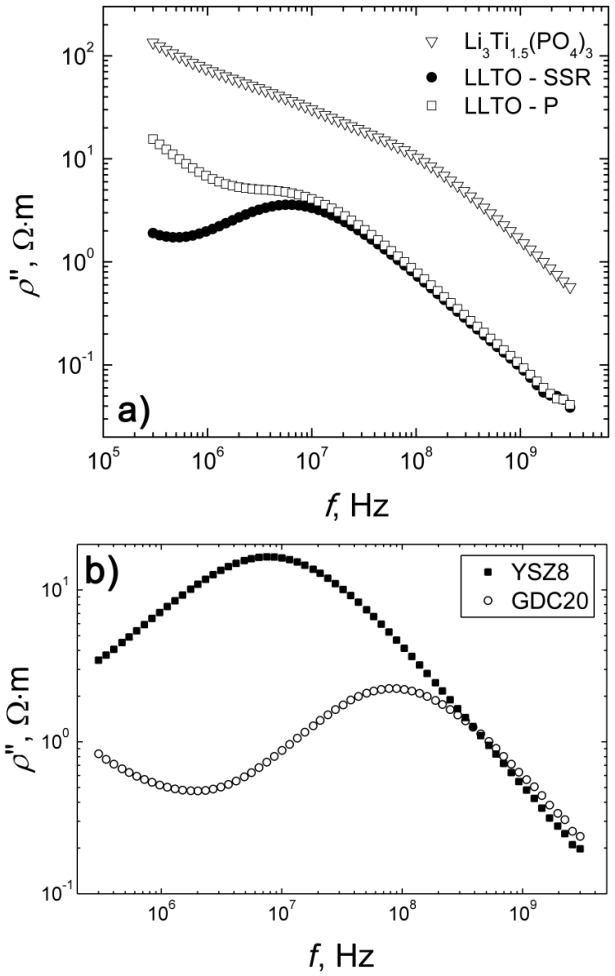

Figure 5: Frequency dependences of imaginary part of impedance of Li^+-conducting ceramics at 300 K (a) and $V_O^{\bullet\bullet}$-conducting ceramics at 700 K (b).

As we can see from the temperature dependences of Maxwell relaxation frequency, it follows Arrhenius law (Fig. 6). The activation energies of f_M (ΔE_f) are presented in Table 2.

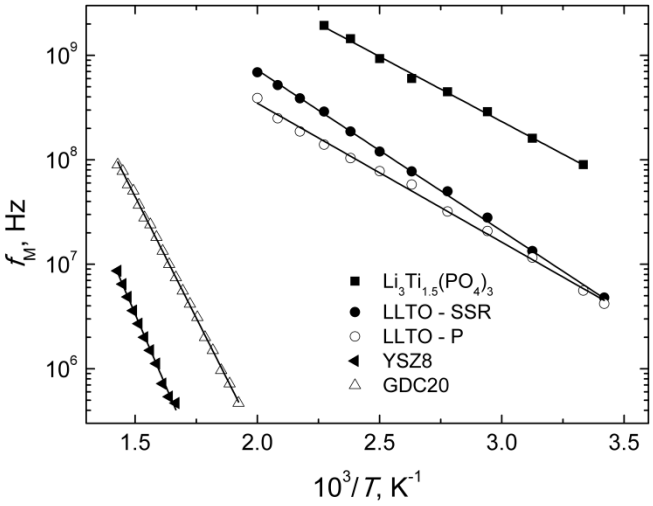

Figure 6: Arrhenius plot of Maxwell relaxation frequency of LLTO, $Li_3Ti_{1.5}(PO_4)_3$, GDC20, and YSZ8 ceramics.

Dielectric permittivity (ε') and dielectric losses ($\tan\delta$) were calculated at the frequency of 1 GHz. This frequency is much higher than Maxwell relaxation frequency in all studied temperatures. At 300 K the values of f_M, ε' and $\tan\delta$ of $Li_3Ti_{1.5}(PO_4)_3$, LLTO, GDC20, and YSZ8 ceramics are summarized in Table 3. Temperature dependences of $\tan\delta$ of $Li_3Ti_{1.5}(PO_4)_3$, LLTO, GDC20, and YSZ8 ceramics are shown in Fig. 7. The increase of the values of ε' with temperature of the investigated compounds can be caused by contribution of the migration polarization of ionic charge carries, vibration of lattice and electronic polarization. The increase of $\tan\delta$ with temperature is related to the contribution of conductivity in the investigated temperature region.

Table 3: ε', $\tan\delta$, f_M of ceramic samples measured at 300 K.

Compound	ε'	$\tan\delta$	f_M, MHz
$Li_3Ti_{1.5}(PO_4)_3$	11	0.12	84
LLTO - SSR	187	0.098	11
LLTO - P	176	0.12	8.6
GDC20	24		
YSZ8	23		

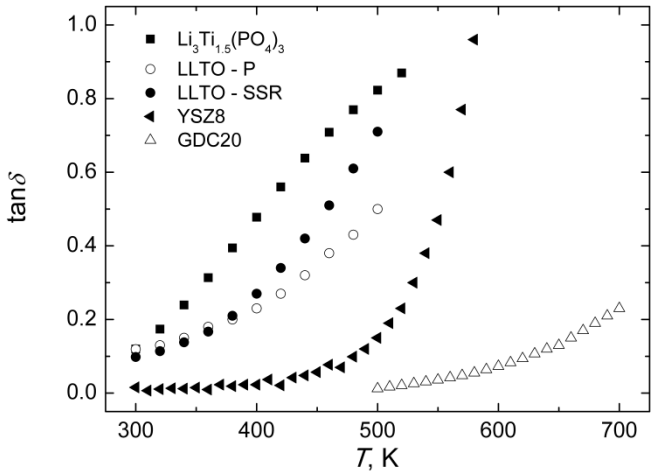

Figure 7: Temperature dependences of dielectric losses of LLTO, $Li_3Ti_{1.5}(PO_4)_3$, GDC20, and YSZ8 ceramics.

4. Conclusions

At room temperature solid electrolyte $Li_3Ti_{1.5}(PO_4)_3$ compound belongs to rhombohedral symmetry (space group $R\bar{3}c$) with six formula units in the unit cell. Dense ceramic samples of $Li_3Ti_{1.5}(PO_4)_3$, $Li_{3x}La_{2/3-x}TiO_3$ (x = 0.12), $Ce_{0.8}Gd_{0.2}O_{1.9}$, and $(ZrO_2)_{92}(Y_2O_3)_8$ have been sintered for electrical investigations. In the frequency range 1 Hz – 1 MHz four-probe method was used to determine total ionic conductivity of the ceramics. In some cases it is difficult to separate total ionic conductivity of the material from the processes appearing in the metal-solid electrolyte interface. Four-probe method gives us the impedance spectra with no contribution of the electrodes used to contact the samples. For the measurements in the microwave range ($3\cdot10^5$-$3\cdot10^9$ Hz) the coaxial line technique was used. The relaxation dispersions in the microwave frequencies have been attributed to ionic relaxation processes in the bulk of ceramics. Temperature dependences of bulk ionic conductivity is caused by ionic mobility in $Li_3Ti_{1.5}(PO_4)_3$, LLTO, GDC20, and YSZ8 compounds which also causes the increase of dielectric losses ($\tan\delta$) with temperature. High measurement frequency of the electrical field (which was much higher than Maxwell relaxation frequency) allowed us to determine dielectric permittivity values of the materials. ε' values of the investigated compounds are caused by contribution of the migration polarization of ionic charge carries, vibration of lattice and electronic polarization.

Acknowledgements

This work was supported by Research Council of Lithuania, Project No. TAP LLT 03/2012.

References

[1] A.G. Belous, G.N. Novitskaya, S.V. Polyanetskaya, Y.I. Gornikov, The crystal-chemical and electrophysical characteristics of the complex oxides $Ln_{2/3-x}M_{3x}TiO_3$, *Russian J. Inorg. Chem.* 32: 156–157, 1987.

[2] Y. Inaguma, Ch. Liquan, M. Itoh, T. Nakamura, T. Uchida, H. Ikuta, M. Wakihara, High ionic conductivity in lithium lanthanum titanate, *Solid State Commun.* 86: 689–693, 1993.

[3] J.L. Fourquet, H. Duroy, M.P. Crosnier-Lopez, Structural and microstructural studies of the series $La_{2/3-x}Li_{3x}\square_{1/3-2x}TiO_3$, *J. Solid State Chem.* 127: 283–294, 1996.

[4] O. Bohnke, J.-C. Badot, J. Emery, Broadband dielectric spectroscopy study of Li^+ ion motions in the fast ionic conductor $Li_{3x}La_{2/3-x}TiO_3$ (x = 0.09); comparison with ^{7}Li NMR results, *J. Phys. Condens. Matter* 15: 7571–7584, 2003.

[5] K. Arbi, J.M. Rojo, J. Sanz, Lithium mobility in titanium based Nasicon $Li_{1+x}Ti_{2-x}(PO_4)_3$ and $LiTi_{2-x}Zr_x(PO_4)_3$ materials followed by NMR and impedance spectroscopy, *J. Eur. Ceram. Soc.* 27: 4215–4218, 2007.

[6] H. Aono, E. Sugimoto, Y. Sadaoka, N. Imanaka, G. Adachi, Ionic conductivity of solid electrolytes based on lithium titanium phosphate, *J. Electrochem. Soc.* 137: 1023–1027, 1990.

[7] P. Bohac, A. Orliukas, L. Gauckler, An improvement of the SOFC performance by electrolyte doping, *Proc. First European Solid Oxide Fuel Cell Forum*, Lucerne, Switzerland, Vol. 2 pp. 651–660, 1994.

[8] O. Bohnke, The fast lithium-ion conducting oxides $Li_{3x}La_{2/3-x}TiO_3$ from fundamentals to application, *Solid State Ionics* 179: 9–15, 2008.

[9] A. Kežionis, E. Kazakevičius, T. Šalkus, A. Orliukas, Broadband high frequency impedance spectrometer with working temperatures up to 1200 K, *Solid State Ionics* 188: 110–113, 2011.

[10] A.Orliukas, P. Bohac, K. Sasaki, L.J. Gauckler, The relaxation dispersion of the ionic conductivity in cubic zirconias, *Solid State Ionics* 72: 35–38, 1994.

[11] A. Orliukas, P. Bohac, K. Sasaki, L. Gauckler, Relaxation dispersion of ionic conductivity in a

$Zr_{0.85}Ca_{0.15}O_{1.85}$ single crystal, *J. Europ. Ceramic Soc.* 12: 87–96, 1993.

[12] R. Sobiestianskas, A. Dindune, Z. Kanepe, J. Ronis, A. Kežionis, E. Kazakevičius, A. Orliukas, Electrical properties of $Li_{1-x}Y_yTi_{2-y}(PO_4)_3$ (where x, $y = 0.3$; 0.4) ceramics at high frequencies, *Materials science and engineering* B 76: 184–192, 2000.

[13] T. Šalkus, A. Dindune, Z. Kanepe, J. Ronis, A. Určinskas, A. Kežionis, A.F. Orliukas, Lithium ion conductors in the system $Li_{1+y}Ge_{2-x-y}Ti_xAl_y(PO_4)_3$ ($x = 0.1 \div 0.3$, $y = 0.07 \div 0.21$), *Solid State Ionics* 178: 1282–1287, 2007.

[14] A.F. Orliukas, T. Šalkus, A. Dindune, Z. Kanepe, J. Ronis, A. Určinskas, E. Kazakevičius, A. Kežionis, V. Kazlauskienė, J. Miškinis, Synthesis, structure and electrical properties of $Li_{1+x+y}Sc_xY_yTi_{2-x-y}(PO_4)_3$ (x=0.15–0.3, y=0.01–0.15) ceramics, *Solid State Ionics* 179: 159–163, 2008.

[15] T. Šalkus, E. Kazakevičius, A. Kežionis, A. Dindune, Z. Kanepe, J. Ronis, J. Emery, A. Boulant, O. Bohnke, A.F. Orliukas, Peculiarities of ionic transport in $Li_{1.3}Al_{0.15}Y_{0.15}Ti_{1.7}(PO_4)_3$ ceramics, *J. Phys.: Condens. Matter* 21: 185502 (7pp), 2009.

[16] M. Gödickemeier, B. Michel, A. Orliukas, P. Bohac, K. Sasaki, L. Gauckler, H. Heinrich, P. Schwander, G. Kostorz, H. Hofmann, O. Frei, Effect of intergranular glass films on the electrical conductivity of 3Y-TZP, *J. Mater. Res.* 9: 1228–1240, 1994.